

INITIAL OPERATION OF SSRL WIGGLER IN SPEAR*

M. Berndt,^a W. Brunk,^a R. Cronin,^b D. Jensen,^a
R. Johnson,^a A. King,^a J. Spencer,^{a,b} T. Taylor,^a and H. Winick^b

I. Summary

A 3λ planar, magnetic wiggler has been designed, built, installed and operated in the SPEAR storage ring. Its primary purpose is to provide tunable synchrotron radiation (SR) with a higher energy and intensity than previously available for a new SR beam line just commissioned at the Stanford Synchrotron Radiation Laboratory. Because the magnet operates from 0-18 kG, it should also produce undulator radiation (UR). Since the wiggler influences storage ring operation in both single beam and colliding beam modes, measurements were made of tune changes, emittance changes and energy spreads which are compared to predictions.¹ Significant improvements in luminosity for high energy physics experiments were observed. The ability to do x-ray experiments easily that were not previously feasible at low electron beam energies and currents has also been demonstrated. We discuss the basic design, some interesting characteristics of the magnetic measurements and our initial operating experience and results.

II. Introduction

Robinson² appears to have been the first to suggest the use of standard wigglers in the straight sections of synchrotrons (or storage rings) to produce SR for experiments. However, except for their use as damping magnets in synchrotrons like CEA,³ there seems to have been little actual use made of them. Among other possibilities, wigglers have also been suggested as a means of optimizing luminosity with decreasing energy in high energy colliding beam experiments.⁴ This is accomplished through blowup of the transverse beam size. The wiggler is also expected to simultaneously improve injection rates by moderating the natural increase in damping times with decreasing energy. Such possibilities show that wigglers are much more than harmonic frequency generators or amplifiers of SR but ion optical devices that can influence many aspects of machine operation in a significant way. Because such effects ultimately determine the usefulness of wigglers as radiation sources, it is necessary to understand them to optimize characteristics such as radiance or spectral radiance.

Although the wiggler can be operated as an undulator (it would produce red light for fields of 350 G and hypothetical beam energies of 500 MeV), its primary purpose is to provide useable x-ray flux when SPEAR is operated between 1.5-2.5 GeV. Since the critical energy of SR produced in a ring bending magnet or standard wiggler is

$$\epsilon_c(\text{keV}) = 2.218 E(\text{GeV})^3 / \rho(\text{m}) = 0.0665 B(\text{kG}) E(\text{GeV})^2$$

and the SPEAR bending radius is 12.7 m one has $(\epsilon_c^W / \epsilon_c^B) \leq 6.86/E(\text{GeV})$ or more than a fourfold increase in critical energy at 1.5 GeV. One also expects a nearly sixfold increase in intensity. Thus, when SPEAR runs as a dedicated SR source, it could be operated at lower energies. Furthermore, when operated for high energy physics, one could still do x-ray experiments that would not otherwise be possible (since the wiggler generally improves luminosity). Because the wiggler

* Work supported by the National Science Foundation in cooperation with the Department of Energy under contract number EY-76-C-03-0515.

^a Stanford Linear Accelerator Center, Stanford University, Stanford, California 94305.

^b Stanford Synchrotron Radiation Laboratory (SSRL).

is tunable and has higher intensity, one also expects a better signal-to-noise ratio. All of the above statements appear to have been verified by the first iron and copper EXAFS spectra taken with SPEAR operating near the ψ resonance (1.5 GeV) under normal colliding beam conditions (4.5 mA).

III. Description

A schematic layout of the SPEAR wiggler is shown in Fig. 1.

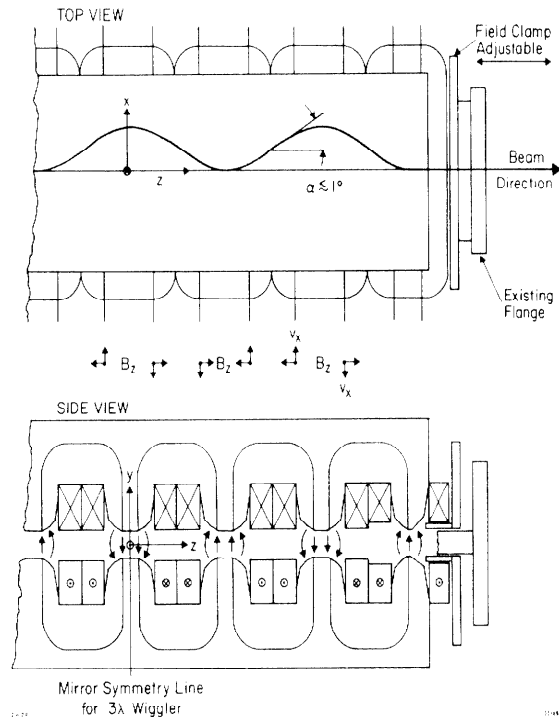


Fig. 1. Schematic layout of SPEAR wiggler showing coordinate conventions and an exaggerated trajectory to illustrate "edge" focusing which is cumulative through the magnet and results in vertical tune shifts Δv_y .

Because it has 3λ , it is mirror symmetric about the x-y and x-z planes. The maximum deflection angle $\alpha \leq 1^\circ$ [$(dx/dz)_{\text{max}}$]. In the dispersion plane (top view), the optical transfer function is equivalent to a drift space since there is no net deflection or displacement of the beam on passing through the wiggler. In the vertical direction (side view) there will be a cumulative focusing effect for particles off the median plane due to the longitudinal field B_z at the entrance and exit of each pole. The effect is cumulative because the field changes sign in synchronism with the transverse velocity v_x ($\approx c dx/dz$). This is illustrated further in Fig. 2 which shows the predicted fields. Mirror symmetry implies $B_z(z, x, 0)$ is identically zero and increases linearly with distance from the median plane so that the wiggler acts like a focusing quadrupole in this direction. Notice that B_z is relatively constant between sign reversals even when the primary fields (B_y) and excitation currents differ considerably between the inner and outer poles. Table I gives the basic parameters.

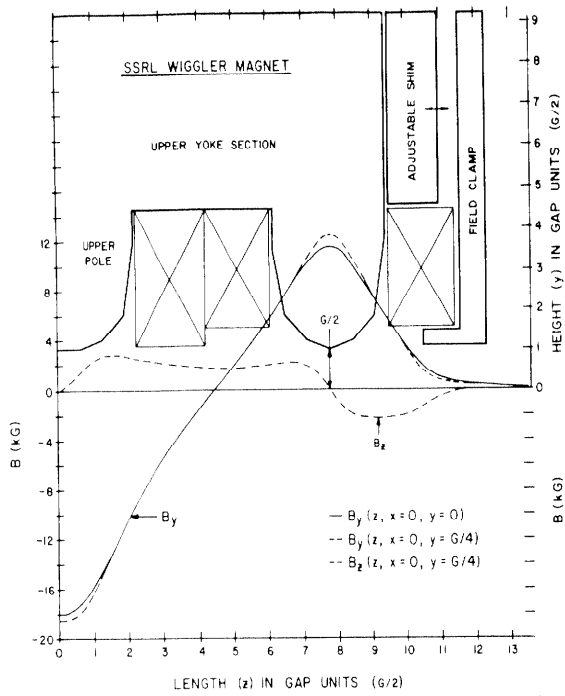


Fig. 2. Layout showing last one and one-half poles in the SPEAR wiggler together with POISSON predictions of the two field components.

Table I - SPEAR Wiggler (3λ) Summary

Number of Poles	7
Maximum Central Induction B_0 (kG)	20
Pole Width w (mm) - Coordinate direction (\hat{x})	304.8
Gap Height G (mm) - Coordinate direction (\hat{y})	41.3
Mechanical Pole Length - Inner (mm) (\hat{z})	88.9
Mechanical Pole Length - Outer (mm) (\hat{z})	66.7
$\frac{1}{2L} \int B_y(x, 0, z) dz$ for $B_0 = 20$ kG (kG-m/kA)	0.576
Effective Magnetic Pole Length - Inner (mm)	98.3
Magnetic Wavelength λ_w (mm)	342.9
Total Magnet Length L (m) - Clamp-to-Clamp	1.219
Amperes for 20 kG	1708
Turns per pole	28
Power (kW) for 20 kG	250
Total Flow Rate (gpm)	42
Maximum Temperature Rise ($^{\circ}C$)	30 $^{\circ}$
Total Magnet Weight (kg)	1100

The disposition of the wiggler near the midpoint of a superperiod in SPEAR is shown in Fig. 3. Because β_x is large, the particle beam size is comparatively large, but the divergence is low ($\sigma_x = 1.33$ mm @ 1.5 GeV, which is comparable to the spreading induced by the oscillatory motion in the wiggler). Because the wiggler is also located at a point of high dispersion in the lattice, the SR more easily excites radial betatron oscillations with the result that high wiggler fields tend to increase the equilibrium beam size. This is why the wiggler is also useful for high energy physics. This would not be the case near the IR unless the basic ring configuration were changed.⁵ A more detailed discussion of such questions is given in Ref. 6.

The physical layout of the SR beam lines and magnets in the vicinity of the wiggler is shown in Fig. 4, and a picture of the actual system is shown in Fig. 5. When operated as an undulator which produces a more collimated beam, one expects to see three bumps dispersed in the horizontal plane corresponding to the upstream bend, the wiggler and downstream bend.

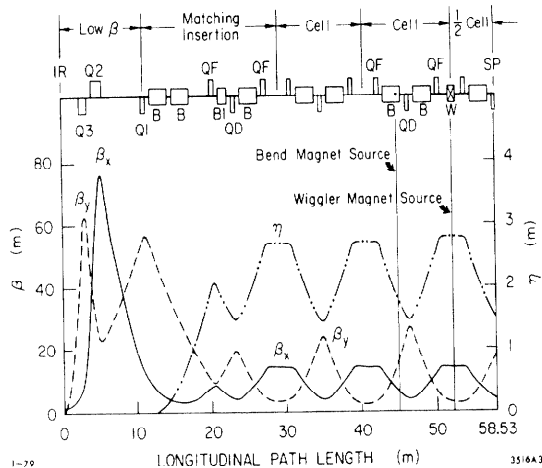


Fig. 3. Layout of one half of a SPEAR superperiod extending from the Interaction Region (IR) to the symmetry Point (SP). The horizontal and vertical betatron amplitude and off-energy function η are shown for tunes used for colliding beam experiments. The wiggler location is labelled W and an adjacent SR source point for beam line III at SSRL is also shown.

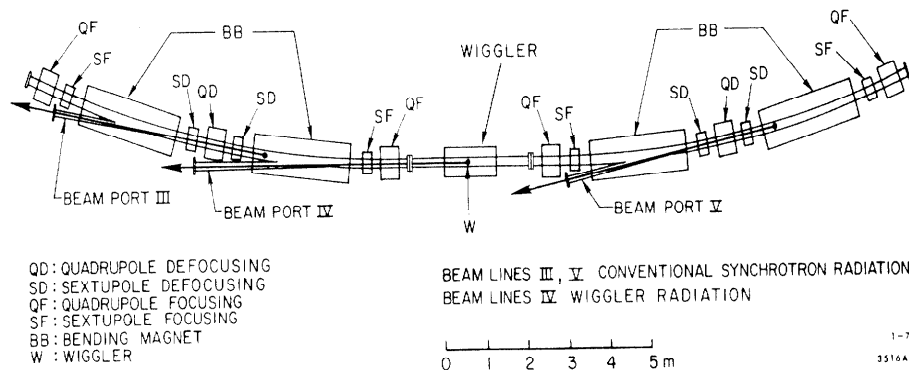


Fig. 4. A more detailed layout in the vicinity of the wiggler showing its location in a straight section of SPEAR and some adjacent SR sources in the ring bending magnets (BB). Note that beam line IV will pass radiation from the wiggler as well as the exit fringing field of the upstream bend and the entrance fringing field of the downstream bend.

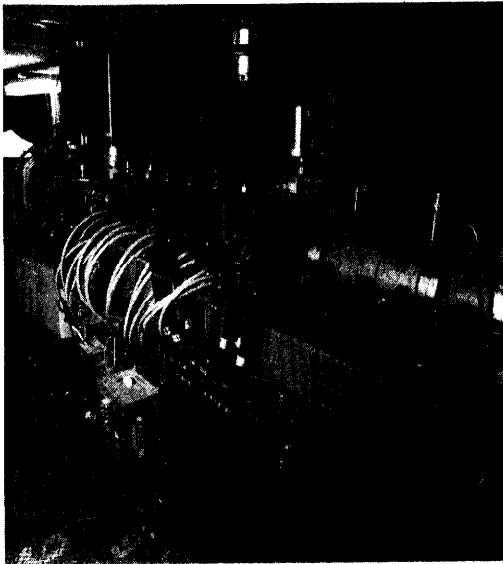


Fig. 5. Picture of wiggler in SPEAR straight section which is shared with beam pickup and feedback modules on either side.

IV. Operation and Results

The wiggler was magnetically measured prior to installation in the ring to check its overall performance as a function of current and determine relative calibration tables for excitation of the inner and out poles which made $fBds=0$. These measurements showed a small but consistent difference between peak fields associated with each polarity with the highest field always associated with the polarity of the center pole. Presumably, this could have been reversed by moving the field clamp, i.e., changing the coupling between poles of opposite polarity. The final calibration tables were determined by tuning the wiggler with beam until there were no net horizontal orbit distortions.

Beam profiles in both transverse directions were measured using SR and fit with Gaussian profiles to determine orbit shifts and size changes with wiggler field. Energy spreading was more difficult to determine. It was measured by looking at the ψ resonance with and without the wiggler. Table II compares some typical results to predictions¹ and Fig. 6 shows the results of the ψ experiment. Since the two runs were done at different times, the apparent downshift in energy should not be compared to predictions⁵ although it is in the right direction. In general, it appears that the effects of the wiggler on storage ring and colliding beam operation is in reasonable agreement with expectations.⁶

Figure 7 shows the wiggler transport line and end station which has just been commissioned. An iron K-edge spectrum (7.2 KeV) taken for calibration at 1.5 GeV during colliding beam operation required only 2 minutes to acquire but would have been impossible without the wiggler. Thus, it appears that wigglers can actually improve both the SR experimental situation as well as that for high energy physics.

Acknowledgements

Many people have contributed to the successful commissioning of the wiggler and its beam line. Mike Adams, Axel Golde, Ron Gould and Ben Salsburg from SSRL and Henry Boatner, Don Burwell, Joe Cobb, John Harris, Joe Jurow and Ewan Paterson from SLAC deserve special mention. The authors also thank Burton Richter

and John Dorfan for discussions and help with obtaining the ψ data as well as Martin Donald, Dick Helm, Martin Lee and Phil Morton for discussion of various subjects.

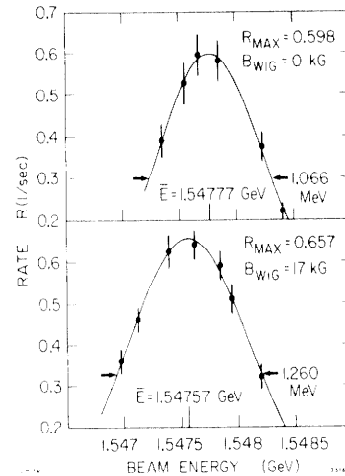


Fig. 6. Reaction rate for events with at least three hadrons in the vicinity of the ψ resonance showing an apparent downshift in energy as well as an increased energy spread due to the wiggler.

Table II - Typical Data

Energy (GeV)	Field (kG)	Measured	Predicted
1.55	10.8	$\Delta v_y = 0.006$	0.004
		$\Delta v_x < 0.001$	0.0
	17.2	$\Delta v_y = 0.012$	0.010
1.88	10.8	$\Delta v_x < 0.001$	0.0
		$(\sigma_E/\sigma_{E_0}) = 1.18$	1.24
	17.2	$\Delta v_y = 0.002$	0.0028
		$\Delta \sigma_x/\sigma_x = 0.9\%$	-0.5%
2.4	16.0	$\Delta v_y = 0.006$	0.0072
		$\Delta \sigma_x/\sigma_x = 3.5\%$	3.1%
	(Luminosity improvement here by > 20%)		
2.4	16.0	$\Delta v_y = 0.003$	0.0036
		$\Delta \sigma_x/\sigma_x = 1.0\%$	-0.57%

References

1. R. H. Helm, PEP Note 272, June 1978.
2. K. W. Robinson, Electron Radiation at 6 BeV, CEA Report #14 (1956).
3. A. Hofmann, R. Little, J. M. Paterson, K. W. Robinson, G. A. Voss and H. Winick, Design and Performance of the Damping System for Beam Storage in the Cambridge Electron Accelerator, Proc. of 6th Int'l. Conf. on High Energy Accelerators CEAL-2000 (September 1967).
4. J. M. Paterson, J. R. Rees and H. Weidemann, Control of Beam Size and Polarization Time in PEP, PEP Report 125 (1975); also in Wiggler Magnets (H. Winick and T. Knight, ed.), SSRP Rept 77/05 (1977).
5. W. Brunk et al., paper presented at this conference.
6. J. E. Spencer and H. Winick, Wiggler Systems as Sources of Electromagnetic Radiation, Chapter in Synchrotron Radiation Research (Plenum Press, New York-London, Editors: S. Doniach and H. Winick).

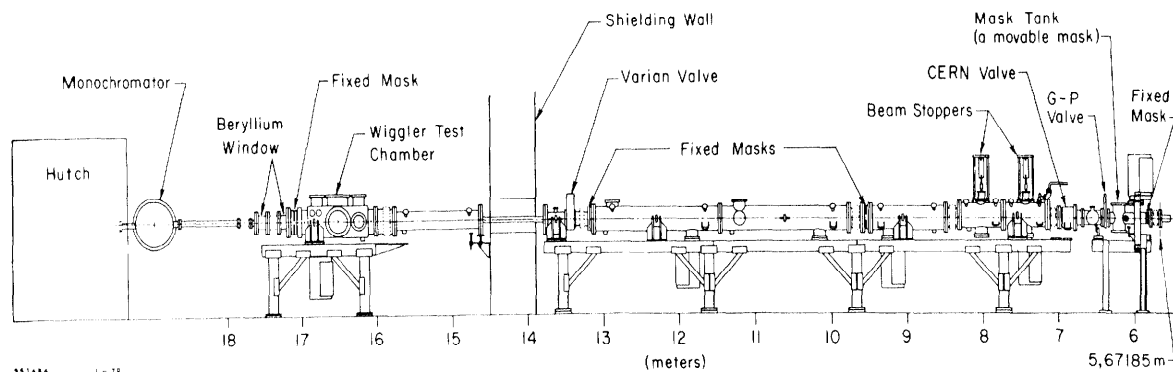


Fig. 7. The transport system begins at the exit of some vacuum plumbing which is part of the SPEAR ring at 5.67 m from the center of the last pole of the wiggler. A bellows mechanically isolates this system followed by a fixed mask with an aperture of 16 mrad horizontally and 2.5 mrad vertically. This is followed by a water cooled movable mask which can be inserted to block beam from an isolation valve (G.P.) or fast acting valve (CERN). The two stoppers are movable stainless steel boxes filled with lead having an effective thickness of 45 cm each. Additional bellows, masks, pumps, valves and spool pieces lead to the shield wall which separates the ring from the experimental area.